scientific reports

Check for updates

OPEN

Regulation of fibronectin and collagens type I, III and VI by TNF-α, TGF-β, IL-13, and tofacitinib

Frederik S. Gillesberg[1,2]✉, Martin Pehrsson[1], Anne-Christine Bay-Jensen[1], Peder Frederiksen[1], Morten Karsdal[1], Bent W. Deleuran[2,3], Tue W. Kragstrup[2,3,4], Satoshi Kubo[5], Yoshiya Tanaka[5] & Joachim H. Mortensen[1]

Understanding how inflammatory cytokines influence profibrogenic wound healing responses in fibroblasts is important for understanding the pathogenesis of fibrosis. TNF-α and IL-13 are key cytokines in Th1 and Th2 immune responses, respectively, while TGF-β1 is the principal pro-fibrotic mediator. We show that 12-day fibroblast culture with TNF-α or IL-13 induces fibrogenesis, marked by progressively increasing type III and VI collagen formation, and that TGF-β1 co-stimulation amplifies these effects. Tofacitinib substantially reduced the formation of ECM proteins in response to IL-13, while fibrogenesis in response to TNF-α or TGF-β1 was marginally inhibited. The in vitro findings were supported by clinical observations in patients with active rheumatoid arthritis, which had elevated serum type III collagen formation, indicating ongoing fibrogenesis during inflammation. After 48–60 weeks of tofacitinib treatment, type III collagen degradation, aswell as formation, were significantly decreased compared to baseline, highlighting dual anti-inflammatory and anti-fibrogenic effects of tofacitinib. In contrast, other anti-inflammatory treatments including methotrexate, adalimumab and tocilizumab demonstrated anti-inflammatory effects only. Our results highlight fibro-inflammatory profiles associated with TNF-α or IL-13 stimulation, both alone and in combination with TGF-β1, and support the use of tofacitinib as an anti-fibrogenic treatment in chronic inflammatory conditions.

Keywords Fibro-inflammation, Fibrosis, Wound healing, Collagen, JAK inhibitor, Tofacitinib

Inflammation is associated with tissue damage and the concomitant induction of wound healing[1,2]. Dysregulated wound healing in the skin serves as a model to understand the pathogenesis of fibrosis across organs. Cutaneous wound healing transitions through a set of regulated phases, including inflammation, proliferation (granulation tissue formation), and remodeling[1,2]. The timely resolution of inflammation is required for the effective transition to repair and tissue regeneration[3]. Non-resolving inflammation prolongs the healing response and can lead to excessive fibroblast activation, ECM synthesis, and eventually fibrosis[3]. Fibrogenesis plays a critical role in the progression of chronic inflammatory diseases such as systemic sclerosis (SSc) and rheumatoid arthritis (RA)[4].

Fibroblasts are ECM-producing cells that become activated in response to cytokines and growth factors during wound healing. During the inflammatory phase, Th1 cytokines such as tumor necrosis factor-α (TNF-α) activate fibroblasts to proliferate, intiating the repair response[5,6]. During the proliferative phase, type 2 cytokines such as interleukin-4 (IL-4) and IL-13 suppress Th1 inflammation, and promote the synthesis of granulation tissue[7]. Transforming growth factor beta 1 (TGF-β1) is a central mediator of repair during all phases of wound healing[8]. TGF-β1 limits inflammation during the early healing response, and regulates myofibroblast differentiation and ECM synthesis during granulation tissue formation and remodeling[8,9]. Fibronectin is the major ECM protein deposited during the inflammatory phase[10], while type III collagen is the major component of granulation tissue[11]. Type VI collagen regulates the assembly of fibrillar collagens and is also expressed at high levels in granulation tissue[12]. Type I collagen gradually becomes the major ECM protein during the remodeling phase, replacing the provisional type III collagen matrix[1]. Biomarkers measuring protein fragments relating to

[1]Nordic Bioscience, Immunoscience, Herlev Hovedgade 205-207, Herlev 2730, Denmark. [2]Department of Biomedicine, Aarhus University, Høegh-Guldbergs Gade 10, Aarhus C 8000, Denmark. [3]Department of Rheumatology, Århus University Hospital, Palle Juul-Jensens Boulevard 99, Aarhus N 8200, Denmark. [4]Diagnostic Center, Regional Hospital Silkeborg, Falkevej 1, Silkeborg 8600, Denmark. [5]The First Department of Internal Medicine, School of Medicine, University of Occupational & Environmental Health, Japan, 1-1 Iseigaoka, Yahata-nishi, 807-8555 Kitakyushu, Japan. ✉email: frg@nordicbio.com

the formation of fibronectin and collagens type I, III and VI may reflect different stages of wound healing, and be used to inform about the pathogenesis of fibrosis.

Janus kinases (JAKs), including JAK1, -2, -3 and TYK2 are cytoplasmic tyrosine kinases that induce pro-inflammatory gene expression in various cells by phosphorylating the signal transducer and activator of transcription (STAT) transcription factors[13]. Tofacitinib is a pan-JAK inhibitor with IC50 of 1 nM, 20 nM and 112 nM against JAK3, JAK2 and JAK1, respectively[14], that effectively reduces inflammation in a wide range of chronic inflammatory diseases[13]. JAK/STAT activation has been reported downstream of TGF-β1 in dermal fibroblasts from SSc patients[15–17] and fibrotic hepatic stellate cells[18]. Tofacitinib has previously been shown to exert anti-fibrogenic effects by inhibiting collagen formation and reducing skin thickening in cell cultures and mice models of SSc[17,19–24]. Additionally, tofacitinib treatment led to clinically significant improvement in the modified Rodnan skin score (mRSS) in a meta-analysis of SSc patients[20].

We hypothesized that prolonged inflammatory cytokine stimulation would synergize with TGF-β1 in fibrogenesis, and that tofacitinib would inhibit collagen formation in response to fibro-inflammation. Co-stimulation with TGF-β1 and IL-13 enhanced type III and VI collagen formation, while TGF-β1 and TNF-α co-stimulation increased fibronectin and type III collagen but reduced type I and VI collagen, compared to TGF-β1 alone. Tofacitinib significantly reduced fibrogenesis induced by IL-13, but had a smaller effect on TNF-α and TGF-β1-induced fibrogenesis. Clinical observations in active RA patients showed elevated type III collagen formation, which decreased after 48–60 weeks of tofacitinib treatment, demonstrating both anti-inflammatory and anti-fibrogenic effects of tofacitinib. These findings support the potential use of tofacitinib as a potential anti-fibrogenic therapy in chronic inflammatory diseases.

Results

IL-13 and TGF-β1 additively promote type III and VI collagen formation, with no change in type I collagen and fibronectin formation

To assess the effect of IL-13 on fibrogenesis, we cultured fibroblasts with IL-13 alone and in combination with TGF-β1 for 12 days. Half-maximal stimulating concentrations were used (supplementary Fig. 1). The formation of collagens type I, -III and -VI and fibronectin were assayed in the fibroblast conditioned media using ELISA. Type I collagen formation started at a high level and decreased over time. TGF-β1 stimulation diminished the reduction in type I collagen over time, while IL-13 did not have any effect on type I collagen formation (Fig. 1A). Type III collagen formation was increased by IL-13 in all donors, and was greater in donor 2 and 4 during co-stimulation with TGF-β1. However, the effect was not equal to the sum of each stimulus, demonstrating a subadditive effect (Fig. 1B). Donor 1 and 3 reached maximum type III collagen formation with respectively TGF-β1 or IL-13 stimulation only, demonstrating no additional effect of combined treatment (Fig. 1B). Type VI collagen formation was additively increased by IL-13 and TGF-β1 in all four donors (Fig. 1C). Fibronectin formation was marginally elevated by IL-13 in donor 1 and 3. TGF-β1 had a major effect on fibronectin levels. There was no additional effect of combined IL-13 + TGF-β1 compared to TGF-β1 alone (Fig. 1D).

Half-maximal stimulation with TNF-α in combination with TGF-β1 do not lead to increased fibrogenesis compared to TGF-β1

To assess the effect of TNF-α on fibrogenesis, we cultured fibroblasts with TNF-α alone and in combination with TGF-β1 for 12 days. Half-maximal stimulating concentrations were used (supplementary Fig. 1). Type I collagen formation was increased with both TNF-α and TGF-β1 stimulation over time compared to vehicle (Fig. 2A). TNF-α increased the formation of type III collagen, but there was no additional effect in combination with TGF-β1 at half-maximal cytokine doses (Fig. 2B). Type VI collagen formation was unchanged with TNF-α from day 0 to 4, but increased from day 4 to day 12 of culture, compared to vehicle. Combined TNF-α + TGF-β1 did not change type VI collagen formation as compared to TGF-β1 only (Fig. 2C). TNF-α stimulation alone decreased fibronectin formation compared to vehicle (Fig. 2D). The combined action of TNF-α + TGF-β1 further increased fibronectin formation in donor 1 and 4, but decreased it in donor 3, compared to TGF-β1 alone. There was no change in donor 2 (Fig. 2D).

Tofacitinib inhibits cytokine induced fibroblast proliferation

Stimulation for 12 days with IL-13, TNF-α or TGF-β1 increased the mitochondrial metabolic activity of fibroblasts, indicating cell proliferation. Proliferation was further increased by co-stimulation with IL-13 + TGF-β1 (Fig. 3A) or TNF-α + TGF-β1 (Fig. 3B), as compared to either stimuli alone. Tofacitinib added in parallel on day four significantly decreased mitochondrial activity in vehicle fibroblasts, aswell as fibroblasts treated with IL-13, TNF-α or TGF-β1. The reduction in metabolic activity achieved with tofacitinib was relatively greater in cytokine-treated fibroblasts compared to vehicle (Fig. 3A-B). Overall, tofacitinib demonstrated a minor cytotoxic effect when used in a dose of 100 nM.

Tofacitinib inhibits cytokine induced formation of type III and VI collagen

In addition to inhibiting cellular proliferation, tofacitinib also had a direct inhibitory effect on the generation of collagens and fibronectin in response to TNF-α, IL-13 and TGF-β1 (Fig. 4, supplementary Figs. 2 & 3). At day 12, tofacitinib had reduced type III and VI collagen formation induced by IL-13, which was consistent across four biological replicates (Fig. 4A–B). Type III formation induced by TGF-β1 as significantly decreased by tofacitinib in donor 2, although a numerical effect was also seen in donor 4 (Fig. 4A & C). Type VI collagen formation induced by TGF-β1 was not decreased by Tofacitinib (Fig. 4B & D). However, tofacitinib decreased type III and VI collagen formation induced by TGF-β1 + IL-13 (Fig. 4B). Type III collagen formation induced by TNF-α was significantly reduced by tofacitinib in donor 2, while tofacitinib reduced type III collagen formation induced by

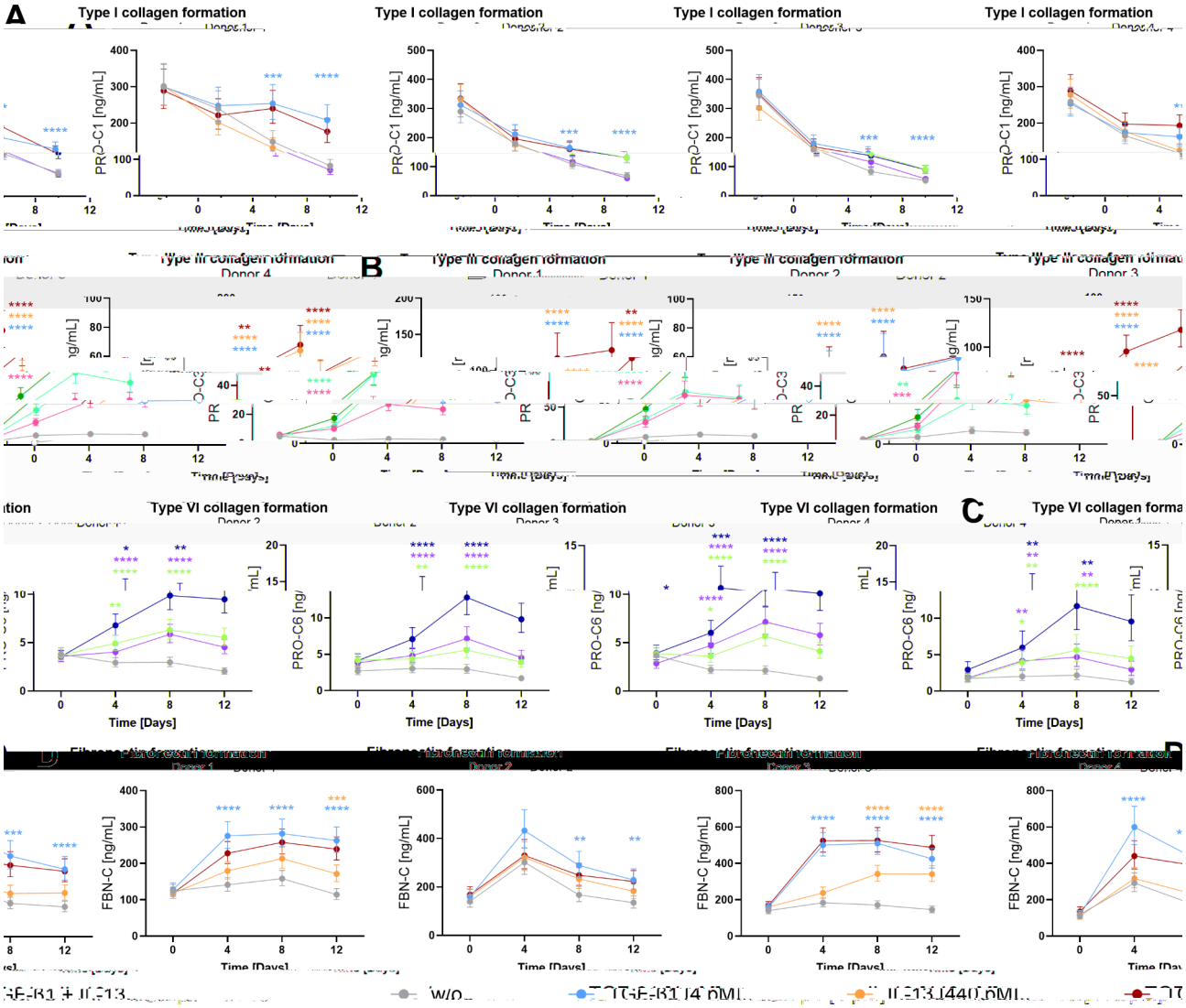

Fig. 1. IL-13 and TGF-β1 cumulatively increase formation of type III and VI collagen. Fibroblasts were treated with TGF-β1 and/or IL-13 for twelve days. **A** Type I collagen formation measured by the PRO-C1 assay. **B** Type III collagen formation measured by the PRO-C3 assay. **C** Type VI collagen formation measured by the PRO-C6 assay. **D** Fibronectin formation measured by the FBN-C assay. Asterisks (*) depict a significant difference compared to vehicle, color coded according to treatment. Fibroblasts treated with IL-13 + TGF-β1 were tested for significance against TGF-β1 alone. $N = 4$ biological replicates shown individually.

TNF-α + TGF-β1 in donor 1, 2 and 4 (Fig. 4C). Type VI collagen formation induced by TNF-α, or a combination of TNF-α + TGF-β1, was significantly reduced in donor 1 and 2 (Fig. 4D).

High doses of TGF-β1 and TNF-α additively promote formation of type III collagen and synergistically promote formation of fibronectin

We additionally investigated the effect of maximum stimulating doses of TNF-α and TGF-β1 on formation collagen and fibronectin (Fig. 5; supplementary Fig. 1). A high TGF-β1 dose sustained type I collagen formation throughout culture to a level comparable to baseline. Type I collagen formation was also sustained by high dose TNF-α, although to a lesser extent than for TGF-β1 (Fig. 5A). Fibroblasts treated with TGF-β1 + TNF-α had reduced type I collagen formation levels compared to TGF-β1 only (Fig. 5A). Fibroblasts treated with TNF-α for four days, followed by crossover to TGF-β1 for eight days, had identical type I collagen formation on day 12 as fibroblasts treated with TGF-β1 only (Fig. 5A). Type III collagen formation was increased to similar levels with TGF-β1 or TNF-α stimulation, respectively, in donor 1, 2 and 4. Donor 3 increased in type III collagen formation levels to a greater degree with TNF-α stimulation (Fig. 5B). Combined TGF-β1 + TNF-α stimulation further increased type III collagen formation. The effect was most pronounced in donor 2 and 4, while the effect was marginal in donor 1 and 3 (Fig. 5B). Fibroblasts treated with TNF-α for four days followed by crossover to TGF-β1 had an increase in type III collagen formation from day 0 to 4, a reduction from day 4 to 8, and a new increase from day 8 to 12 (Fig. 5B). A high TNF-α dose did not increase type VI collagen formation compared

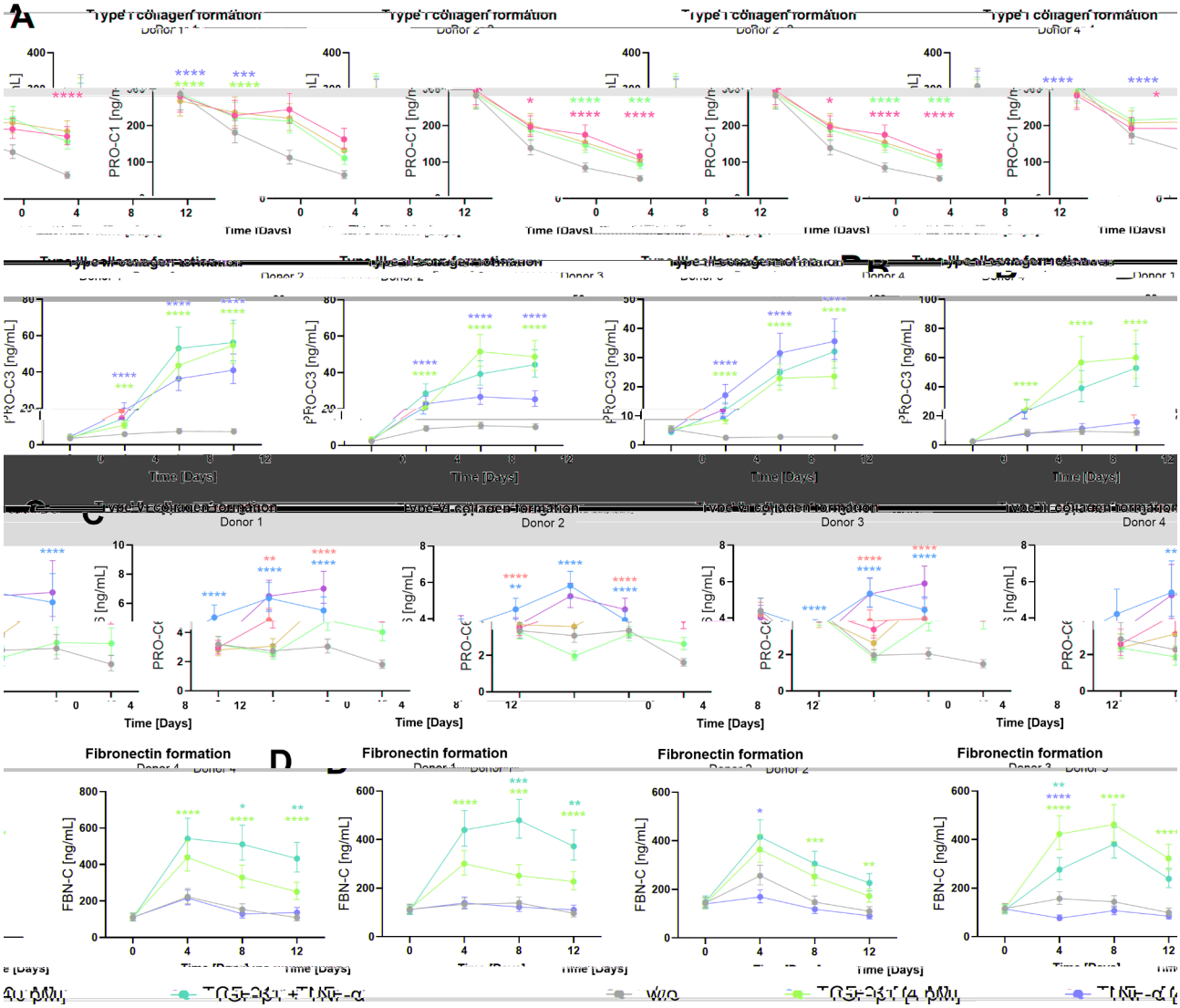

Fig. 2. The effect of half-maximal stimulating doses of TNF-α and TGF-β1 on ECM formation. **A** Type I collagen formation measured by the PRO-C1 assay. **B** Type III collagen formation measured by the PRO-C3 assay. **C** Type VI collagen formation as measured by the PRO-C6 assay. (D) Fibronectin formation measured by the FBN-C assay. Asterisks (*) depict a significant difference of treatment compared to vehicle, with color code. Fibroblasts treated with TNF-α + TGF-β1 were tested for significance against TGF-β1 alone. $N = 4$ biological replicates shown individually.

to vehicle, although two donors increased from day 8 to 12 (Fig. 5C). Fibroblasts treated with TGF-β1 + TNF-α throughout culture had reduced type VI collagen formation compared to fibroblasts treated with TGF-β1 alone (Fig. 5C). Treatment with TNF-α prior to TGF-β1 led to a greater type VI collagen formation level on day 12 compared to TGF-β1, which was consistent across four donors (Fig. 5C). TNF-α stimulation alone decreased fibronectin formation compared to vehicle (Fig. 5D). However, the combination of high dose TGF-β1 + TNF-α synergistically increased fibronectin formation compared to TGF-β1 stimulation (Fig. 5D). Fibroblasts treated with TNF-α for four days followed by crossover to TGF-β1 had increased levels of fibronectin formation on day 12 compared to TGF-β1 treatment (Fig. 5D).

Picrosirius red staining of decellularized matrices

The deposition of collagen into plate wells were assessed using picrosirius red staining. Sirius red is known to stain both type I and III collagen fibers. On day 12, plate wells were decellularized, allowing qualitative assessment of deposited collagen. Sirius red staining was greatest in fibroblast wells conditioned with TGF-β1, or with TNF-α followed by TGF-β1 (Fig. 6A). As type I collagen formation measured by PRO-C1 was highest for these conditions (Fig. 6B), picrosirius red appeared to stain mostly deposited type I collagen fibers (Fig. 6B).

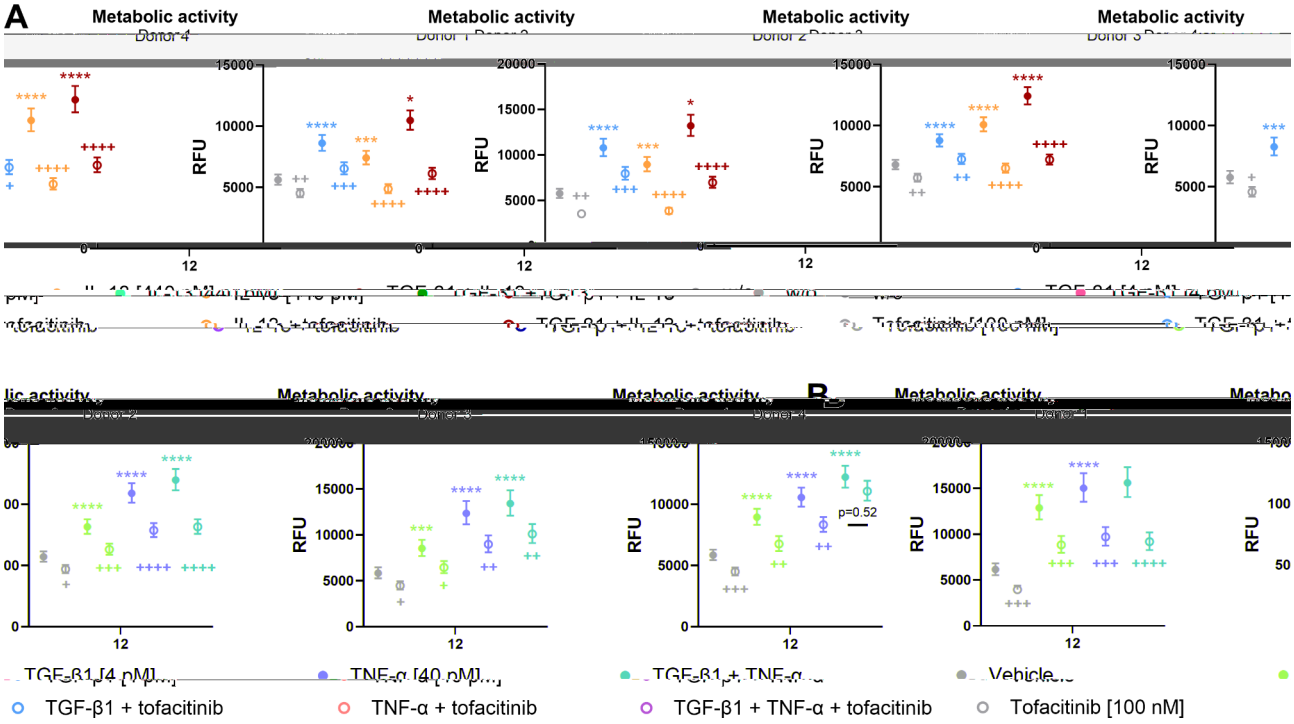

Fig. 3. Tofacitinib inhibits cytokine-induced fibroblast proliferation. **A** Metabolic activity on day 12 in fibroblasts treated with IL-13 and/or TGF-β1. In parallel treatments, Tofacitinib was added from day four of culture. **B** Metabolic activity on day 12 in fibroblasts treated with TNF-α and/or TGF-β1 for twelve days. In parallel treatments, Tofacitinib was added from day four of culture. Asterisks (*) are color coded and denote a significant contrast of treatment compared to vehicle; fibroblasts treated with IL-13 + TGF-β1 or TNF-α + TGF-β1 were compared to TGF-β1. Crosses (+) are color coded and denote significant contrasts of tofacitinib compared to the parallel treatment without tofacitinib. $N = 4$ biological replicates shown individually.

Type III collagen formation is reduced by tofacitinib in patients with active rheumatoid arthritis

The soluble biomarkers measured in fibroblast cultures may also be measured systemically in patients with chronic inflammation to monitor fibrogenesis. Type III collagen degradation (C3M) and type III collagen formation (PRO-C3) was evaluated at baseline and after 48–60 weeks in 149 RA patients initiating treatment with respectively methotrexate (MTX, $n = 23$), adalimumab (ADA, $n = 49$), tofacitinib (TOFA, $n = 27$) or tocilizumab (TCZ, $n = 50$). Baseline characteristics of the patients is summarized in Table 1. The mean age was similar between groups. The MTX group included newly diagnosed patients, which had a shorter disease duration, as well fewer bone erosions as assessed by the sharp-van der heijde erosion (SvdHS) score. The TOFA group was characterized by higher disease activity by DAS28CRP, CDAI, HAQ-DI compared to the other groups. All treatments were associated with a reduction in systemic type III collagen degradation (C3M) after 48–60 weeks, indicating decreased inflammation (Fig. 7A). However, Tofacitinib treatment also led to a reduction in fibrogenesis, as type III collagen formation (PRO-C3) was significantly decreased at 48–60-week follow-up compared to baseline ($p < 0.05$) (Fig. 7B). In contrast, patients treated with MTX or TCZ had a relative increase in PRO-C3, while there was no change with ADA (Fig. 7B). Thus, JAK-STAT inhibition reduced tissue degradation resulting from inflammation, but additionally had an inhibiting effect on systemic fibrogenesis in RA patients.

Discussion

In the present study we aimed to investigate the fibrogenic behavior of fibroblasts cultured in an environment mimicking chronic inflammation. We demonstrate that prolonged stimulation of dermal fibroblasts with TNF-α or IL-13 induced fibrogenesis characterized by type III and VI collagen formation, which progressively increased over a culture period of twelve days. The effect on collagen formation was further amplified when combined with TGF-β1. Tofacitinib substantially reduced the fibrogenic response to IL-13, while the anti-fibrogenic effects were minor against TNF-α or TGF-β1 alone. In the context of TNF-α and TGF-β1 co-stimulation, tofacitinib moderately inhibited collagen formation. Our in vitro findings were supported by clinical observations in patients with active rheumatoid arthritis, where elevated systemic type III collagen formation indicated ongoing fibrogenesis due to inflammation. Notably, tofacitinib inhibited collagen formation after 48–60 weeks of treatment, while other anti-inflammatory treatments, including methotrexate, adalimumab and tocilizumab did not demonstrate an anti-fibrogenic effect. Thus, tofacitinib was the only treatment that demonstrated a combined anti-inflammatory and anti-fibrotic effect.

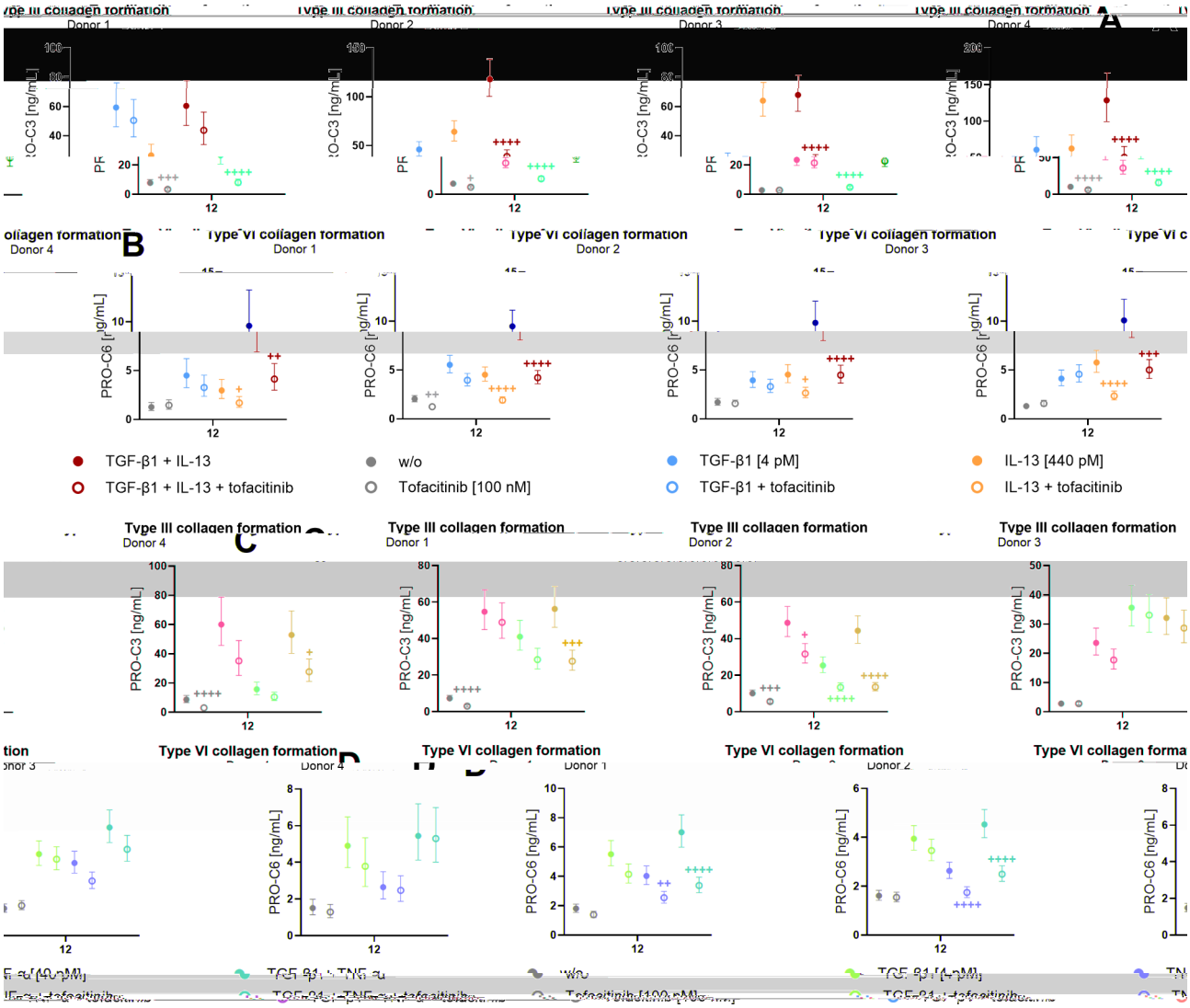

Fig. 4. Tofacitinib inhibits the formation of type III and VI collagen. The effect of tofacitinib was investigated in fibroblasts treated with IL-13 and/or TGF-β1, aswell as TNF-α and/or TGF-β1 for twelve days. In parallel treatments, Tofacitinib was added from day four of culture. Panel **A** and **C**: Type III collagen formation measured by the PRO-C3 assay on day twelve of culture. Panel **B** and **D**: Type VI collagen formation measured by the PRO-C6 assay on day twelve of culture. Crosses (+) are color coded and denote a significant contrast of tofacitinib compared to the parallel treatment without tofacitinib. $N=4$ biological replicates shown individually.

We assessed fibrogenesis by measuring soluble biomarkers quantifying key ECM components present during wound healing, including type I, -III, and -VI collagens and fibronectin. Fibronectin and collagens type III and VI are major constituents of granulation tissue, which is deposited during active fibrogenesis in wound healing. In our proposed model (Fig. 8), the proliferative response of wound healing is extended during sustained cytokine stimulation, leading to excessive deposition of granulation tissue. Over time, the deposited granulation tissue may be replaced by stiff type I collagen matrix, leading to fibrosis.

A profibrogenic role of IL-13 is well-described in the literature, promoting collagen synthesis directly in fibroblasts[7]. Meanwhile, most in vitro evidence point to a direct anti-fibrotic effect of TNF-α on fibroblasts, inhibiting myofibroblast differentiation and collagen formation[25–28]. Our results support an anti-fibrotic role of TNF-α, in the sense that type I collagen formation was decreased by TGF-β1 + TNF-α co-stimulation compared to TGF-β1 alone. Interestingly however, the formation of fibronectin and type III collagen was increased by TGF-β1 + TNF-α co-stimulation compared to TGF-β1 alone. Thus, rather than being anti-fibrogenic, TNF-α altered the ECM profile of TGF-β1 to promote early granulation tissue formation. This is in line with one report describing a pro-fibrogenic role of TNF-α, where subcutaneous TNF-α perfusion for seven days led to growth of a tissue mass consisting of fibroblasts, new capillaries and irregularly deposited collagen[29], resembling granulation tissue.

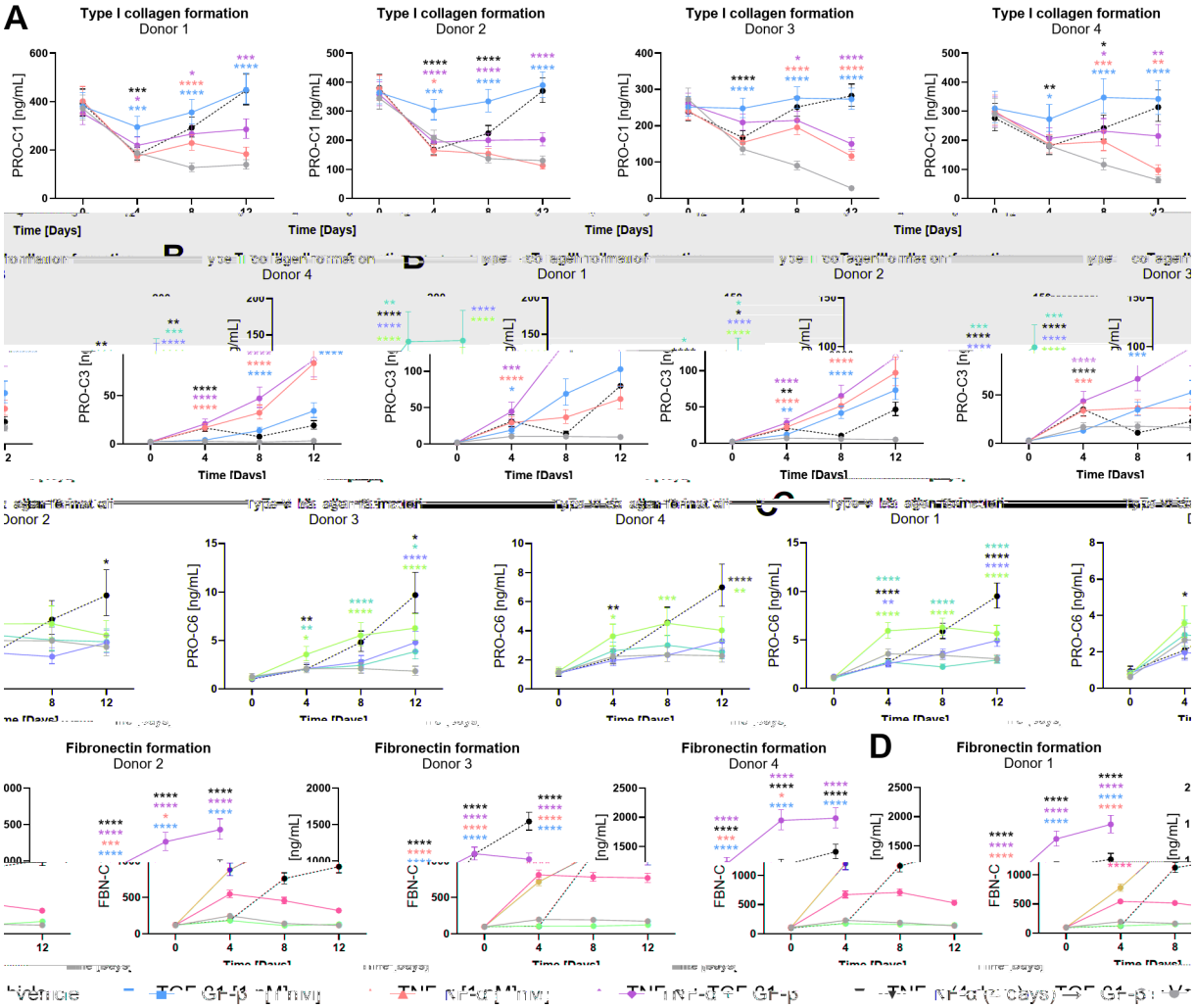

Fig. 5. High doses of TGF-β1 and TNF-α additively promote the formation of type III collagen, and synergistically promote fibronectin formation. **A** Type I collagen formation measured by the PRO-C1 assay. **B** Type III collagen formation measured by the PRO-C3 assay. **C** Type VI collagen formation measured by the PRO-C6 assay. **D** Fibronectin formation measured by the FBN-C assay. Asterisks (*) depict a significant difference of treatment compared to vehicle, with color code. Fibroblasts treated with TGF-β1 + TNF-α, aswell as TNF-α for four days followed by TGF-β1, were tested for a significance aagainst TGF-β1 only. $N = 4$ biological replicates shown individually.

The Scar-in-a-Jar model is an in vitro fibroblast model developed for anti-fibrotic drug screening[30]. We investigated whether Tofacitinib could inhibit collagen formation directly in our experimental system. Anti-fibrogenic effects of tofacitinib have been reported previously[17,19–24]. We used Tofacitinib in a dose of [100 nM] which was slightly cytotoxic as judged by metabolic activity. Tofacitinib substantially reduced the effect of IL-13 on collagen formation, constitent with the effects of IL-13 being dependent on JAK/STAT signaling. IL-13 binds the IL-4/IL-13 receptor complex in fibroblasts, leading to activation of JAK1/2 and TYK2, followed by STAT6 phosphorylation and pro-fibrotic gene expression[7]. The fibrogenic profile induced by TNF-α and TGF-β1 in this system appeared to be primarily driven by other pathways than the JAK/STAT pathway. The canonical TGF-β signaling pathway in fibroblasts is the Smad pathway, where phosphorylation of Smad2 and Smad3 proteins drive ECM synthesis[9]. TNF-α activates the NF-κB and MAPK (mitogen-activated protein kinase) pathways in fibroblasts[31], but may activate JAK-STAT signaling indirectly through autocrine secondary mediators, such as platelet-derived growth factor[6,32]. NF-κB signaling downstream of TNF-α has previously been shown to inhibit SMAD2/3 activation in response to TGF-β1 in dermal fibroblasts[25,26,33]. In the context of TGF-β1 and TNF-α co-stimulation, fibroblasts may become more sensitive to JAK inhibition due to NF-κB interference with the SMAD pathway.

While our study demonstrates that tofacitinib inhibits fibroblast activity, its primary anti-fibrogenic effect may arise from reducing the release of cytokines and growth factors by immune cells[24]. Cytokines such as TGF-β1, TNF-α, and IL-13, which drive fibrogenesis, are in large part produced by immune cells. Therefore, tofacitinib's main anti-fibrotic action may stem from lowering the cytokine concentration that reaches fibroblasts, rather than directly interfering with pro-fibrotic signaling in these cells.

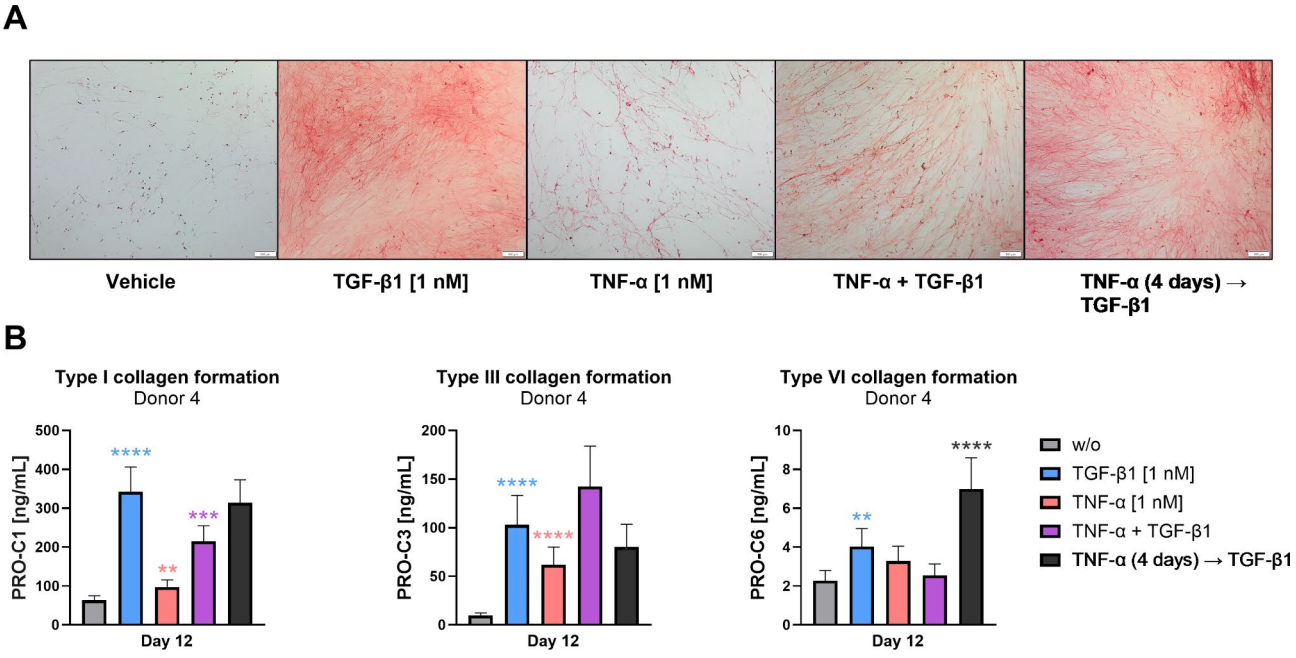

Fig. 6. Picrosirius red staining of decellularized matrices from fibroblasts treated with TGF-β1 and TNF-α. Pictures depict results from one representative donor. **A** Collagen staining by picrosirius red. Pictures were taken at 10X magnification in the center of plate wells. Scale bar: 100 µM (bottom right). **B** Type I, III and VI collagen formation quantified by soluble biomarkers in the representative donor on the same day as staining.

	MTX (baseline) $n = 23$	ADA (baseline) $n = 49$	TOFA (baseline) $n = 27$	TCZ (baseline) $n = 50$
Age, years	55.4 (SD 13.17)	61.3 (SD 11.1)	53.3 (SD 12.6)	56.3 (SD 18.5)
Male, %	21.7	12.2	14.8	12.0
Disease duration, months	6.4 (SD 2.4)	95.5 (SD 112)	75.8 (SD 81.4)	153 (SD 136)
Synthetic DMARD-naïve, %	100	0	0	0
Biologic DMARD-naïve, %	100	83	100	40
DAS28CRP	3.60 (SD 0.9)	4.66 (SD 1.2)	5.59 (SD 1.2)	4.84 (SD 1.2)
CDAI	14.3 (SD 6.7)	24.0 (SD 14.7)	34.9 (SD 13.2)	25.7 (SD 12.9)
SDAI	15.2 (SD 7.8)	26.6 (SD 15.1)	37.2 (SD 14.3)	27.8 (SD 13.8)
HAQ-DI	0.59 (SD 0.5)	1.11 (SD 0.7)	1.46 (SD 0.7)	1.46 (SD 0.9) (2 missing)
ES	2.1 (SD 3.1) (2 missing)	35.5 (SD 53.9)	26.3 (SD 31.7)	59.5 (SD 72.3)
JSN	3.3 (SD 4.6) (2 missing)	26.9 (SD 36.1)	26.9 (SD 26.9)	49.3 (SD 42.6)
SvdHS	4.9 (SD 7.3)	62.4 (SD 89.5)	53.2 (SD 57.9)	108.8 (SD 114)
C3M, ng/ml	16.4 (SD 10.4)	13.3 (SD 6.3)	18.4 (SD 11.4)	16.7 (SD 10.9)
Pro-C3, ng/ml	15.3 (SD 4.8)	20.4 (SD 14.4)	19.9 (SD 6.4)	18.6 (SD 11.1)

Table 1. Baseline characteristics of rheumatoid arthritis patients treated with methotrexate (MTX), Adalimumab (ADA), Tofacitinib (TOFA) or Tocilizumab (TCZ).

This study has limitations. The fibroblasts proliferated to a different extent in response to TNF-α, TGF-β1 and IL-13, as assessed by mitochondrial metabolic activity. The increase in biomarker levels, particularly of type III collagen formation measured by PRO-C3, may reflect cellular proliferation, rather than increased synthesis from individual fibroblasts. Moreover, the formation levels assessed by soluble biomarkers may not correlate with the actual deposition of collagen and fibronectin into the ECM. Our model is based on the scar-in-a-jar setup, where fibroblasts are cultured on plastic with Ficoll[30]. The addition of Ficoll provides a macromolecular crowding effect, enabling the complete biosynthetic cascade of collagen maturation, deposition and cross-linking[30,34]. However, this setup cannot replicate the complexity of a true three-dimensional environment. Moreover, plastic is an extremely stiff matrix that does not represent elastic tissues such as skin. Plastic has a strong influence on fibroblast phenotype, being associated with the generation of α-SMA myofibroblasts[35]. It should be mentioned that we cultured fibroblasts in DMEM containing high glucose. Hyperglycemia has been reported to directly promote collagen formation in cultured fibroblasts through activation of the extracellular regulated kinase

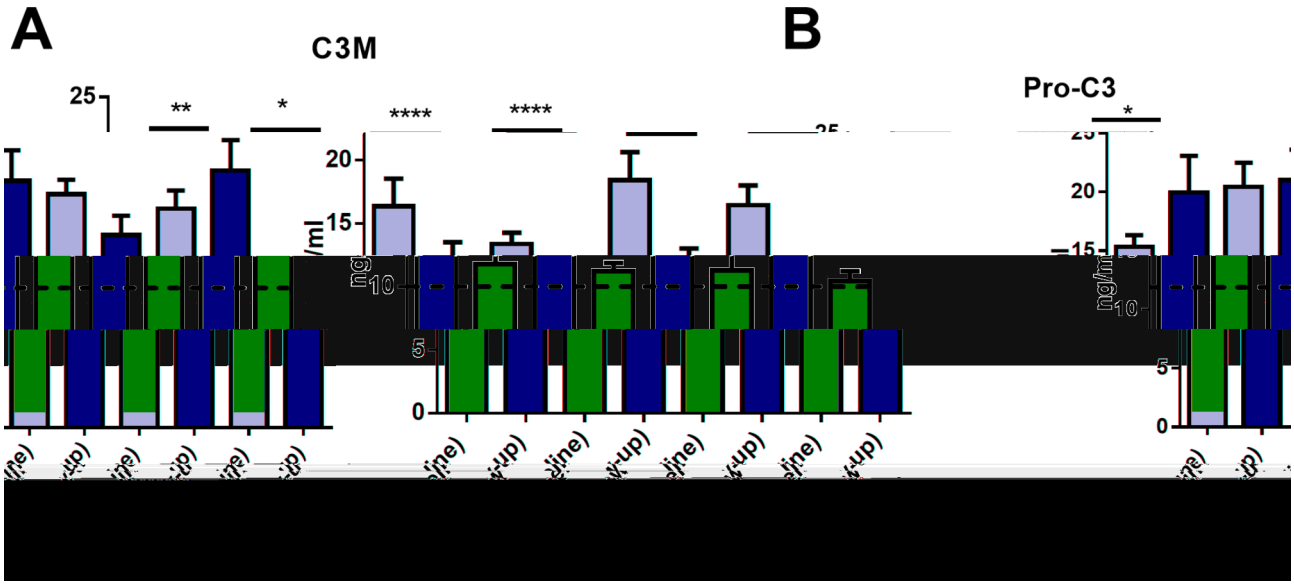

Fig. 7. Tofacitinib is anti-inflammatory and anti-fibrogenic in rheumatoid arthritis patients. **A** Serum C3M levels reflecting degradation of type III collagen due to inflammation, before and after 48–60 weeks of treatment with methotrexate, adalimumab, tofacitinib or tocilizumab. **B** Serum PRO-C3 levels reflecting formation of type III collagen, before and after 48–60 weeks of treatment with methotrexate, adalimumab, tofacitinib or tocilizumab. Dotted lines represent healthy reference levels in serum for C3M (10 ng/mL) and PRO-C3 (12 ng/mL). Bar plots are shown as mean + SEM.

(ERK)[36]. It is not known whether in vivo fibrosis is associated with a local hyperglycemic environment. Finally, a high dose of ascorbic acid was used to promote collagen formation, which may not reflect the in vivo availability of ascorbic acid. These experimental conditions may limit the translational value of our results.

In conclusion, fibro-proliferative responses were initiated during twelve-day fibroblast culture with TNF-α or IL-13, characterized by formation of type III and VI collagen. These responses were further increased by TGF-β1 co-stimulation. Fibroblast activity due to fibro-inflammation was inhibited by tofacitinib in vitro and in RA patients with active inflammation.

Materials and methods

Cell culture

Primary healthy human dermal fibroblasts were purchased from Lonza (Adult CC-2511, Lonza). Skin samples were acquired by Lonza from breast reduction surgeries with patients written informed consent. The fibroblasts were expanded to passage 7 prior to experiments. Cells were expanded in standard incubation conditions (37 °C, 5% CO_2) in Dulbecco's modified Eagle medium (DMEM) with GlutaMAX and high glucose (Gibco, cat#10566016), additionally supplemented with 1% penicillin/streptomycin (P/S, Sigma-Merck, cat#P4333) and 10% fetal bovine serum (FBS, Sigma-Merck, cat#F7524). At 80% confluency, cells were brought into suspension using EDTA-supplemented trypsin (Sigma-Merck, cat#T3924) and counted using NucleoCounter NC-202 (ChemoMetec). 30.000 cells/well were seeded in 48-well culture plates in 10% FBS culture media. After seeding for 24 h, the cells were serum starved in 0.4% FBS culture media for 24 h. The day following starvation was defined as 'day 0'. From day 0, the cells were cultured for 12 days in 0.4% FBS culture media supplemented with Ficoll PM400 [38 mg/mL] (Cytvia, cat#17030050) and Ficoll PM70 [56 mg/mL] (Cytvia, cat#17031005) and 0.5 mg/mL L-ascorbic acid (Fujifilm Wako, cat#013-12061). Treatments included TNF-α (Sigma-Merck, cat#SRP3177), TGF-β1 (R&D Systems, cat#240-B), IL-4 (R&D Systems, cat#204-IL), IL-13 (R&D systems, cat#213-ILB) and Tofacitinib citrate (Sigma-Merck, cat#PZ0017). Cells cultured without treatment (unstimulated) were used as vehicle control. Conditioned media was changed every 4 days and stored at -20°C for biomarker measurements.

Metabolic activity assay

Mitochondrial activity was measured using the alamarBlue™ assay (Invitrogen, cat#DAL1025) as a surrogate measure for cell viability. The assay is based on the reduction of resazurin to resorufin due to mitochondrial respiration, producing a red flourescent color. Cells were incubated in 0.4% FBS culture media containing 10% AlamarBlue stock solution for 2 h at 37 °C, 5% CO2. Following incubation, the conditioned media from plate wells was transferred to a 96-well black plate (Sigma-Merck, cat. CLS3915), and the fluorescence intensity in the media was determined using 540 nM as excitation and 590 nM as emission wavelengths.

ELISA

Biomarkers for the formation of collagens and fibronectin were measured in the fibroblast conditioned media on day 0, 4, 8 and 12 using competitive ELISAs (Nordic Bioscience). Formation of Type I, III and VI collagen and

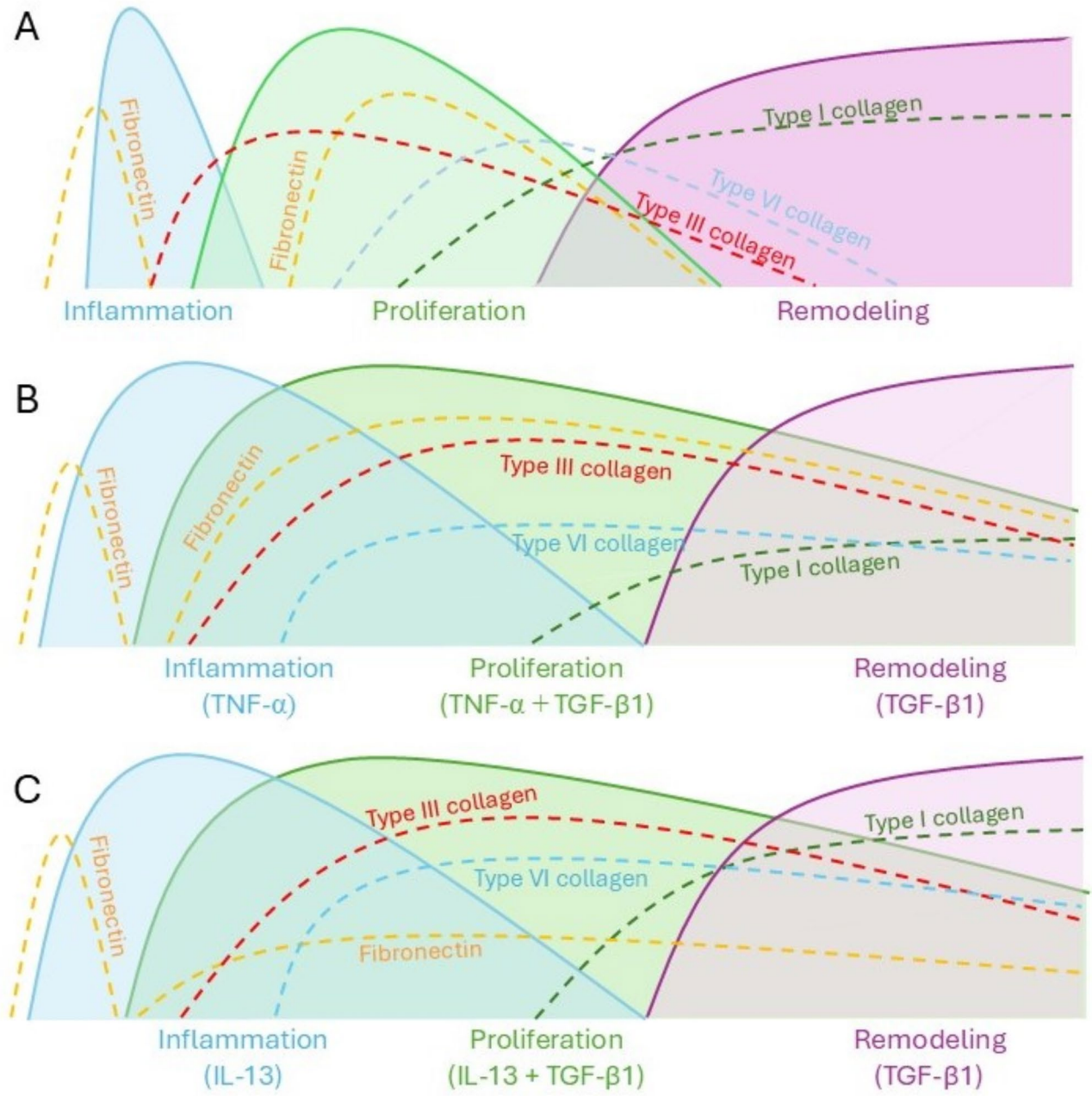

Fig. 8. Proposed model of how the investigated biomarkers relate to wound healing. **A** Phsyiological wound healing consists of three phases, including inflammation, proliferation and remodeling. Different ECM components, including fibronectin and collagens type I, III and VI peak during different phases. The phases of inflammation and proliferation are temporally restricted to restore tissue integrity. **B** Sustained TNF-α stimulation prolongs the proliferative phase of wound healing, resulting in greater formation of fibronectin and type III collagen, while type I collagen is reduced. **B** Sustained IL-13 stimulation prolongs the proliferative phase, resulting in greater type III and VI collagen formation. Type I collagen formation is unchanged. A prolonged phase of granulation tissue formation may result in fibrosis.

fibronectin was quantified using the nordicPRO-C1[37], nordicPRO-C3[38], nordicPRO-C6[39] and nordicFBN-C[40] assays, respectively. Samples below the lower limit of detection was assigned the value for the lower limit of blank (LLOB) for the corresponding assay. The PRO-C1 assay measures the unique epitope ^{96}'PDGSESPTDQETTGV'^{110} found in the N-terminal propeptide of type I collagen α1 (COL1A1) chain[37]. The PRO-C3 assay measures the unique neo-carboxy-terminal epitope ^{145}'CPTGPQNYSP↓'^{153} of the N-terminal propeptide of type III collagen α1 (COL3A1) chain, that is generated following maturation of type III collagen by N-proteinase (ADAMTS2)[38]. The PRO-C6 assay the measures the C-terminus of the type VI collagen α3 (COL6A3) chain, with the unique

sequence $_{3168}$'KPGVISVMGT'^{3177} [39]. The FBN-C assay measures the C-terminal of fibronectin with the unique sequence ^{2467}'VQADREDSRE'$_{2477}$ [40]. C3M was measured in serum samples from rheumatoid arthritis patients. C3M measures a neoepitope fragment ^{591}'KNGETGPQGP'^{602} produced after matrix metalloproteinase 9 (MMP9) cleavage within mature type III collagen α1 (COL3A1) chain[41], reflecting connective tissue inflammation.

Picrosirius Red staining of decellularized matrices

Culture plate wells were decellularized as described previously[42]. Briefly, cells were rinsed 3 times in dulbecco's phosphate buffered saline (PBS, Sigma-Merck, cat#D8537) and lysed in PBS containing 20 mM NH_4OH (Honeywell, cat# 15628370) and 0.5% Triton-X100 (Sigma-Merck, cat#X100). After lysis, the cellular debris was diluted in PBS and stored at 4 °C overnight. The next day, decellularized matrices were rinsed two times in PBS, followed by rinsing two times in PBS supplemented with 1 mM $CaCl_2$ and 1 mM $MgSO_4$. Decellularized matrices were stained for 1 h with sirius red solution, consisting of 0.1% w/v sirius red dye (VWR, cat#B21693) diluted in a saturated aqueous solution of picric acid (Sigma-Merck, cat#19737). After staining, the plate wells were dehydrated stepwise with 70%, 96% and 99% ethanol (VWR Chemicals). Each dehydration step was carried out for 2 min. Pictures were taken using brightfield microscopy at the center of plate wells immediately after dehydration.

Rheumatoid arthritis patients

In total, 149 RA patients from University Hospital of Occupational and Environmental Health, Japan, were included in the study; 23 received MTX, 49 initiated ADA, 27 initiated TOFA, 50 initiated TCZ. Patients treated with MTX, ADA and TCZ were consecutively registered under the clinical practice setting (MTX was initiated during July 2011 and January 2013; ADA was initiated during August 2008 and March 2010; TCZ was initiated during March 2008 and October 2010), while patients treated with TOFA were under both domestic and global clinical trial setting before approval by Japan's National Health Insurance System (NHI) (TOFA was initiated during March 2008 and February 2010). Clinical parameters including tender joint count 28 (TJC28), swollen joint count 28 (SJC28), patients' global health (PGH), patients' global assessment (PGA), evaluators' global assessment (EGA), C-reactive protein (CRP), and erythrocyte sedimentation rate (ESR), to calculate disease activity score in 28 joints (DAS28), DAS28-CRP, clinical disease activity index (CDAI), and simplified disease activity index (SDAI), were evaluated and blood samples were taken at baseline and 48–60 weeks later (follow-up). The study was performed in accordance with the Helsinki Declaration and with approval from the ethics committee of the University Hospital of Occupational and Environmental Health, Japan (approval number: 10–114). All patients provided written informed consent.

Statistics and graphical representation

In vitro studies

For dose-titration studies, GraphPad Prism (version 10.2.3) was used calculate the area under curve (AUC) values for each technical replicate (3–4 replicates) over twelve days of stimulation. This was done for 4 biological replicates of primary dermal fibroblasts. GraphPad Prism was subsequently used to perform four parameter logistic regression and calculate cytokine EC50 doses for each biomarker (supplementary Fig. 1). Other analyses were conducted in R, version 4.2 together with RStudio version 2024.04.1 + 748.

In the studies with repeated biomarker measurements, the biomarkers were log-transformed to achieve variance homogeneity across time, and subsequently fitted to a linear mixed model using the lme4 package[43]. Model fitting and testing was performed individually on biological donors, specifying a random effect for technical replicate (3–4 technical replicates per donor). In this way, the effect of treatment on the technical replicates in specific donors could be investigated. Modeling was based on a $2\times2\times2\times4$ factorial design, using levels of individual cytokines (IL-13/TNF-α and TGF-β1), tofacitinib and time as explanatory factors. The emmeans package was used to estimate mean biomarker values at each time point[44]. Pairwise comparisons at each time point were used to test for differences in means. All pairwise comparisons were two-tailed tests. A significant contrast was specified at an alpha level of 0.05. Sidak's method was used to control the type I error rate for pairwise comparisons. In Fig. 5, the fit was based on a 5×4 factorial design, using Treatment and Time as explanatory factors. Subsequent pairwise comparisons were adjusted with Tukey's method.

Metabolic activity on day 12 measured by alamar blue was fitted to a linear model using a $2\times2\times2$ factorial design, using individual cytokines (IL-13/TNF-α and TGF-β1) and tofacitinib as explanatory factors. Pairwise comparisons were done using two-tailed tests with an alpha level of 0.05. Multiple comparisons were adjusted with Sidak's method.

Statistical analyses made in R were plotted in GraphPad Prism as shown in the results section. All plots are depicted as geometric mean ± 95% confidence interval, unless otherwise stated. Asteriks (*) or crosses (+) on graphs depict significant contrasts: * $p<0.05$, ** $p<0.01$, *** $p<0.001$, **** $p<0.0001$.

Rheumatoid arthritis patients

Wilcoxon matched pairs signed rank test was used to compare baseline biomarker concentrations with follow-up levels. The statistical analysis was done with MedCalc Statistical Software version 14.8.1. Biomarker results were plotted in GraphPad Prism. Asteriks (*) on graphs depict significant contrasts: * $p<0.05$, ** $p<0.01$, *** $p<0.001$, **** $p<0.0001$.

Data availability

Primary- and and processed data will be provided upon request to the corresponding author.

Received: 15 August 2024; Accepted: 20 December 2024

Published online: 07 January 2025

References

1. Darby, I. A., Laverdet, B., Bonté, F. & Desmoulière, A. Fibroblasts and myofibroblasts in wound healing. *Clin. Cosmet. Investig. Dermatol.* **7**, 301–311 (2014).
2. Soliman, A. M. & Barreda, D. R. Acute inflammation in tissue healing. *Int. J. Mol. Sci.* **24**, 641 (2022).
3. El Ayadi, A., Jay, J. W. & Prasai, A. Current approaches targeting the wound healing phases to attenuate fibrosis and scarring. *Int. J. Mol. Sci.* **21**, 1105 (2020).
4. Henderson, N. C., Rieder, F. & Wynn, T. A. Fibrosis: from mechanisms to medicines. *Nature* **587**, 555–566 (2020).
5. Ritsu, M. et al. Critical role of tumor necrosis factor-α in the early process of wound healing in skin. *J. Dermatology Dermatologic Surg.* **21**, 14–19 (2017).
6. Battegay, E. J., Raines, E. W., Colbert, T. & Ross, R. TNF-alpha stimulation of fibroblast proliferation. Dependence on platelet-derived growth factor (PDGF) secretion and alteration of PDGF receptor expression. *J. Immunol.* **154**, 6040–6047 (1995).
7. Allen, J. E. IL-4 and IL-13: regulators and effectors of wound repair. *Annu. Rev. Immunol.* **41**, 229–254 (2023).
8. Pakyari, M., Farrokhi, A., Maharlooei, M. K. & Ghahary, A. Critical role of transforming growth factor beta in different phases of wound healing. *Adv. Wound Care* **2**, 215–224 (2013).
9. Hu, B., Wu, Z. & Phan, S. H. Smad3 mediates transforming growth factor-β–induced α-smooth muscle actin expression. *Am. J. Respir. Cell Mol. Biol.* **29**, 397–404 (2003).
10. Patten, J. & Wang, K. Fibronectin in development and wound healing. *Adv. Drug Deliv. Rev.* **170**, 353–368 (2021).
11. Alhajj, M. & Goyal, A. *Physiology, Granulation Tissue*. *StatPearls* (2022).
12. Oono, T. et al. Expression of type VI collagen mRNA during wound healing. *J. Invest. Dermatol.* **100**, 329–334 (1993).
13. Liu, J., Wang, F. & Luo, F. The role of JAK/STAT pathway in fibrotic diseases: molecular and cellular mechanisms. *Biomolecules* **13**, 119 (2023).
14. Changelian, P. S. et al. Prevention of organ allograft rejection by a specific Janus kinase 3 inhibitor. *Science (80-.).* **302**, 875–878 (2003).
15. Dees, C. et al. JAK-2 as a novel mediator of the profibrotic effects of transforming growth factor β in systemic sclerosis. *Arthritis Rheum.* **64**, 3006–3015 (2012).
16. Chakraborty, D. et al. Activation of STAT3 integrates common profibrotic pathways to promote fibroblast activation and tissue fibrosis. *Nat. Commun.* **8**, 1130 (2017).
17. Damsky, W. et al. Jak inhibition prevents Bleomycin-induced fibrosis in mice and is effective in patients with Morphea. *J. Invest. Dermatol.* **140**, 1446-1449.e4 (2020).
18. Tang, L.-Y. et al. Transforming Growth Factor-β (TGF-β) directly activates the JAK1-STAT3 axis to induce hepatic fibrosis in coordination with the SMAD pathway. *J. Biol. Chem.* **292**, 4302–4312 (2017).
19. McGaugh, S., Kallis, P., De Benedetto, A. & Thomas, R. M. Janus kinase inhibitors for treatment of morphea and systemic sclerosis: A literature review. *Dermatol. Ther.* **35**, e15437 (2022).
20. Moriana, C., Moulinet, T., Jaussaud, R. & Decker, P. JAK inhibitors and systemic sclerosis: A systematic review of the literature. *Autoimmun. Rev.* **21**, 103168 (2022).
21. Wang, W. et al. The JAK/STAT pathway is activated in systemic sclerosis and is effectively targeted by tofacitinib. *J. Scleroderma Relat. Disord.* **5**, 40–50 (2020).
22. Karatas, A. et al. Tofacitinib and metformin reduce the dermal thickness and fibrosis in mouse model of systemic sclerosis. *Sci. Rep.* **12**, 2553 (2022).
23. Aung, W. W. et al. Immunomodulating role of the JAKs inhibitor tofacitinib in a mouse model of bleomycin-induced scleroderma. *J. Dermatol. Sci.* **101**, 174–184 (2021).
24. Lescoat, A. et al. Combined anti-fibrotic and anti-inflammatory properties of JAK-inhibitors on macrophages in vitro and in vivo: Perspectives for scleroderma-associated interstitial lung disease. *Biochem. Pharmacol.* **178**, 114103 (2020).
25. Distler, J. H. W., Schett, G., Gay, S. & Distler, O. The controversial role of tumor necrosis factor α in fibrotic diseases. *Arthritis Rheum.* **58**, 2228–2235 (2008).
26. Goldberg, M. T., Han, Y.-P., Yan, C., Shaw, M. C. & Garner, W. L. TNF-α suppresses α-smooth muscle actin expression in human dermal fibroblasts: an implication for abnormal wound healing. *J. Invest. Dermatol.* **127**, 2645–2655 (2007).
27. Mauviel, A. et al. Tumor necrosis factor inhibits collagen and fibronectin synthesis in human dermal fibroblasts. *FEBS Lett.* **236**, 47–52 (1988).
28. Chizzolini, C. et al. Systemic sclerosis Th2 cells inhibit collagen production by dermal fibroblasts via membrane-associated tumor necrosis factor α. *Arthritis Rheum.* **48**, 2593–2604 (2003).
29. Piguet, P. F., Grau, G. E. & Vassalli, P. Subcutaneous perfusion of tumor necrosis factor induces local proliferation of fibroblasts, capillaries, and epidermal cells, or massive tissue necrosis. *Am. J. Pathol.* **136**, 103–110 (1990).
30. Chen, C. et al. The Scar-in-a-Jar: studying potential antifibrotic compounds from the epigenetic to extracellular level in a single well. *Br. J. Pharmacol.* **158**, 1196–1209 (2009).
31. Sabio, G. & Davis, R. J. TNF and MAP kinase signalling pathways. *Semin. Immunol.* **26**, 237–245 (2014).
32. Vignais, M.-L., Sadowski, H. B., Watling, D., Rogers, N. C. & Gilman, M. Platelet-derived growth factor induces phosphorylation of multiple JAK family kinases and STAT proteins. *Mol. Cell. Biol.* **16**, 1759–1769 (1996).
33. Bitzer, M. et al. A mechanism of suppression of TGF–β/SMAD signaling by NF-κB/RelA. *Genes Dev.* **14**, 187–197 (2000).
34. Puerta Cavanzo, N., Bigaeva, E., Boersema, M., Olinga, P. & Bank, R. A. Macromolecular crowding as a tool to screen anti-fibrotic drugs: the Scar-in-a-Jar system revisited. *Front. Med.* **7**, 1–14 (2021).
35. Avery, D. et al. Extracellular matrix directs phenotypic heterogeneity of activated fibroblasts. *Matrix Biol.* **67**, 90–106 (2018).
36. Tang, M. et al. High glucose promotes the production of collagen types I and III by cardiac fibroblasts through a pathway dependent on extracellular-signal-regulated kinase 1/2. *Mol. Cell. Biochem.* **301**, 109–114 (2007).
37. Leeming, D. J. et al. Enzyme-linked immunosorbent serum assays (ELISAs) for rat and human N-terminal pro-peptide of collagen type I (PINP) — assessment of corresponding epitopes. *Clin. Biochem.* **43**, 1249–1256 (2010).
38. Nielsen, M. J. et al. The neo-epitope specific PRO-C3 ELISA measures true formation of type III collagen associated with liver and muscle parameters. *Am. J. Transl. Res.* **5**, 303–315 (2013).
39. Sun, S. et al. Collagen type III and VI turnover in response to long-term immobilization. *PLoS One* **10**, 1–14 (2015).
40. Bager, C. L. et al. Quantification of fibronectin as a method to assess ex vivo extracellular matrix remodeling. *Biochem. Biophys. Res. Commun.* **478**, 586–591 (2016).
41. Barascuk, N. et al. Development and validation of an enzyme-linked immunosorbent assay for the quantification of a specific MMP-9 mediated degradation fragment of type III collagen—A novel biomarker of atherosclerotic plaque remodeling. *Clin. Biochem.* **44**, 900–906 (2011).
42. Franco-Barraza, J., Beacham, D. A., Amatangelo, M. D. & Cukierman, E. Preparation of extracellular matrices produced by cultured and primary fibroblasts. *Curr. Protoc. Cell Biol.* **71**, 10.9.1–10.9.34. (2016).
43. Bates, D., Mächler, M., Bolker, B. & Walker, S. Fitting linear mixed-effects models using lme4. *J. Stat. Softw.* **67**(1), 1–48 (2015).
44. Lenth, R. emmeans: Estimated Marginal Means, aka Least-Squares Means. R package version 1.10.3, https://CRAN.R-project.org/package=emmeans (2024).

Author contributions

The design of the work was done by Frederik S. Gillesberg, Martin Pehrsson and Joachim H. Mortensen, Satoshi Kubo and Yoshiya Tanaka. Data acquisition was performed by Frederik S. Gillesberg, Satoshi Kubo and Yoshiya Tanaka. Data analysis was performed by Frederik S. Gillesberg, Martin Pehrsson and Joachim H. Mortensen and Peder Frederiksen. Peder Frederiksen is the main contributor to the statistical analysis of the data. Frederik S. Gillesberg drafted the manuscript. Martin Pehrsson, Anne-Christine Bay-Jensen, Morten Karsdal, Satoshi Kubo, Yoshiya Tanaka, Bent W. Deleuran, Tue W. Kragstrup substantially revised the work. The submitted version of the manuscript was approved by all authors.

Declarations

Competing interests

Martin Pehrsson, Anne-Christine Bay-Jensen, Morten Karsdal, Peder Frederiksen and Joachim H. Mortensen are employees at Nordic Bioscience, Denmark. Nordic Bioscience is a biotechnology company doing contract research with the pharmaceutical industry. Anne-Christine Bay-Jensen and Morten Karsdal own stock in Nordic Bioscience. The biomarker assays PRO-C1, PRO-C3, PRO-C6, FBN-C and C3M are proprietary intellectual property of Nordic Bioscience. Frederik S. Gillesberg, Bent W. Deleuran, Tue W. Kragstrup, Satoshi Kubo and Yoshiya Tanaka have no competing interests in relation to this work.

Additional information

Supplementary Information The online version contains supplementary material available at https://doi.org/10.1038/s41598-024-84151-3.

Correspondence and requests for materials should be addressed to F.S.G.

Reprints and permissions information is available at www.nature.com/reprints.

Publisher's note Springer Nature remains neutral with regard to jurisdictional claims in published maps and institutional affiliations.